Philosophical Magazine Letters

ISSN: 0950-0839 (Print) 1362-3036 (Online) Journal homepage: https://www.tandfonline.com/loi/tphl20

Structural, elastic, electronic, phonon and thermal properties of Ir_3Ta and Rh_3Ta alloys

N. Arikan, O. Örnek, Ş. Uğur & G. Uğur

To cite this article: N. Arikan, O. Örnek, Ş. Uğur & G. Uğur (2015) Structural, elastic, electronic, phonon and thermal properties of Ir_3Ta and Rh_3Ta alloys, Philosophical Magazine Letters, 95:7, 392-400, DOI: 10.1080/09500839.2015.1076175

To link to this article: https://doi.org/10.1080/09500839.2015.1076175

Philosophical Magazine Letters, 2015
Vol. 95, No. 7, 392–400, http://dx.doi.org/10.1080/09500839.2015.1076175

Taylor & Francis
Taylor & Francis Group

Structural, elastic, electronic, phonon and thermal properties of Ir_3Ta and Rh_3Ta alloys

N. Arikan[a]*, O. Örnek[b], Ş. Uğur[c] and G. Uğur[c]

[a]*Eğitim Fakültesi, İlköğretim Bölümü, Ahi Evran Üniversitesi, 40100, Kırşehir, Turkey;* [b]*Mühendislik-Mimarlık Fakültesi, Metalürji ve Malzeme Mühendisliği Bölümü, Ahi Evran Üniversitesi, 40100 Kırşehir, Turkey;* [c]*Fen Fakültesi, Fizik bölümü, Gazi Üniversitesi, 06500 Ankara, Turkey*

(*Received 26 March 2015; accepted 15 July 2015*)

We have studied the structural, elastic, electronic, phonon and thermodynamic properties of Ir_3Ta and Rh_3Ta alloys, using *ab initio* calculations. For the $L1_2$ phase, we report the calculated lattice constants, bulk modulus and elastic constants, and these values are compared with previously published values. We also derive the elastic constants from the values of the slopes of the acoustic branches in the phonon dispersion curves. The band structures show that both materials are metallic. The phonon dispersion curves, and their corresponding total and projected densities of states, are obtained using a linear response in the framework of the density functional perturbation theory. The specific heat capacity at constant volume and different temperatures is calculated, and this aspect is discussed using the quasi-harmonic approximation.

Keywords: *ab initio*; band calculations; density-functional theory; electronic density of states; electronic structure; first-principles calculations; phonons

Introduction

In recent years, there have been significant studies of Ir-based and Rh-based alloys, as they have garnered importance as ultra-high-temperature structural materials because of their high melting point, high-temperature strength, and excellent oxidation and corrosion resistance [1–3]. The Ir_3Ta and Rh_3Ta alloys of $L1_2$ phase are widely used in gas turbine engines, fusion reactors and space-based power systems. Recently, several groups have studied the structural, mechanical, elastic, electronic, thermodynamic, phase transition and thermal properties of Ir_3Ta and Rh_3Ta alloys, employing different experimental and theoretical methods [4–29]. Watanabe et al. [4] measured the crystal structure of an Ir-Ta alloy film that changed from fcc-Ir to Ir_3Ta, then to α-(Ir-Ta), Ta_3Ir, and finally bcc-Ta with increasing Ta content. Huang et al. [5] determined the creep properties at high temperature of Ir_3Ta alloys. Miura et al. [15] measured the mechanical properties of Rh_3Ta and showed that it has a weak positive temperature dependence of strength at around 1273 K, which is about half the melting point for this alloy. Experimentally, there are reports of Ir_3Ta and

*Corresponding author. Email: narikan@ahievran.edu.tr

Rh_3Ta, as high-temperature structural materials, stabilizing in the Cu_3Au-type cubic structure. For high-temperature applications, Nuttens et al. [7] measured the Rh_3Ta alloy that was formed between 800 and 900 °C, and showed that this can be used as a diffusion barrier for temperatures lower than 825 °C. The elastic properties of Rh_3Ta were investigated using the tight-binding (TB) and linear augmented plane wave methods by Chen et al. [8]. Terada et al. [9–11] measured the thermal expansion and thermal conductivity of Ir_3Ta and Rh_3Ta alloys in the temperature range of 300–1100 K. Their results indicated that both materials have a large thermal conductivity and a small thermal expansion. Yu et al. [12] measured the phase transition and phase composition of Ir_3Ta alloy using an energy dispersive analysis X-ray spectroscopy system attached to a scanning electron microscope. The electronic structures of the Ir_3Ta and Rh_3Ta $L1_2$ intermetallic alloys have been studied by means of the self-consistent tight-binding linear muffin tin orbital (TB-LMTO) method [13,14].

The aim of this article is to provide a comparative study of the structural, elastic, electronic, vibration and thermodynamic properties of Ir_3Ta and Rh_3Ta alloys using the density functional theory. To our knowledge, the phonon properties of Ir_3Ta and Rh_3Ta alloys in the $L1_2$ phase have not yet been calculated or measured.

Method

The calculations were performed using a plane-wave pseudopotential scheme, within the density functional theory, as implemented in the Quantum-ESPRESSO (QE) code [30] and Vienna *ab initio* Simulation Package (VASP) code [31,32]. We have chosen the exchange-correlation potential, as approximated by the generalized gradient approximation (GGA) of Perdew–Burke–Ernzerhof [33] for QE and Perdew–Zunger [34] parameterization of the local density approximation (LDA) for VASP [35,36]. Plane-wave energy cut-offs of 544 and 260 eV were used in QE and VASP calculation, respectively. The k-points samplings were $10 \times 10 \times 10$ for QE and $5 \times 5 \times 5$ for VASP in the Brillouin zone for Ir_3Ta and Rh_3Ta, respectively, according to the Monkhorst–Pack scheme [37]. The structure was relaxed until the convergence in energy of $1.0\ \text{eV} \times 10^{-5}$ eV was reached. Integration up to the Fermi surface has been performed using the smearing technique [38] with smearing parameter $\sigma = 0.272$ eV for QE. In the VASP calculations, the Methfessel–Paxton smearing [38] with broadening of 0.225 eV was used for relaxation. We calculated the phonon spectra, using both the linear response method [39,40] and the direct method [41] described within the supercell approach. For the linear response theory, we calculated eight dynamical matrices, on a $4 \times 4 \times 4$ q-point mesh, to obtain complete phonon dispersions and vibrational density of states. For the direct method, the force constants are determined from the Hellmann–Feynman forces induced by the displacement of an atom in the $2 \times 2 \times 2$ supercell. Generation of the Hellmann–Feynman forces was made by displacing the asymmetric atoms from their equilibrium positions with amplitude ±0.02 Å. The temperature dependence of the constant volume specific heat was calculated using the quasi-harmonic approximation (QHA) [42].

Results

We calculated the ground-state lattice parameters of Ir_3Ta and Rh_3Ta alloys and compared these with the available experimental and theoretical values [8,13,22, 24–27]. Table 1 lists the computed values of lattice constants, bulk moduli, shear moduli, elastic constants and *B/G* ratios for the Ir_3Ta and Rh_3Ta alloys. As can be clearly seen, the lattice constant of Ir_3Ta is higher than that of Rh_3Ta, which can be explained by the fact that the atomic radius of Ir is higher than that of Rh atom: R (Ir) = 1.87 Å > R (Rh) = 1.83 Å. The calculated values of bulk modulus, shear modulus and elastic constants of Ir_3Ta are larger than those of Rh_3Ta, on account of a higher atomic radius difference between the constituent atoms for both alloys. The calculated lattice constants from LDA are in better agreement with the experiment values than those calculated by GGA. Our calculated values for both alloys are in good agreement with the available data. The elastic constants, C_{ij}, are valuable parameters for understanding how a material behaves based on its structural stability and ductility properties. There are three independent elastic constants (C_{11}, C_{12} and C_{44}) in cubic crystals. The conditions of stability reduce to a simple form: $C_{11} > C_{12} > 0$, $C_{44} > 0$ and $C_{11} - C_{12} > 0$. We have used these procedures for the calculation of elastic constants and bulk modulus in a previous publication [43,44]. Unfortunately, there are no experimental data available in the literature regarding the elastic constants of these materials. Our calculated values for the bulk modulus and elastic constants for Ir_3Ta are less than those calculated by Chen et al. [22]. For Rh_3Ta, the bulk modulus and elastic constants are larger than those obtained by Chen et al. [8]. Our results show very good agreement with the values obtained by Ould Kada et al. [28]. Chen et al. [8,22] calculated the shear moduli for Ir_3Ta and Rh_3Ta

Table 1. Computed lattice constants (Å), bulk modulus (GPa), elastic constants (GPa), shear modulus (GPa) and and *B/G* for Ir_3Ta and Rh_3Ta in $L1_2$ phase.

Compounds	References	a	B	C_{11}	C_{12}	C_{44}	G	B/G
Ir_3Ta	This work (GGA)	3.934	326.117	535.391	221.48	252.427	214.244	1.522
	This work (LDA)	3.867	373.20	583.18	268.20	282.66	223.53	1.669
	VASP-GGA [22]	3.884	391.11	665.32	259.01	311.31	259.74	1.505
	Exp. [24]	3.889						
	Exp. [27]	3.886						
	[29]		319					
Rh_3Ta	This work (GGA)	3.910	264.224	414.692	188.99	183.498	155.239	1.702
	This work(LDA)	3.830	311.35	479.08	227.48	210.14	171.05	1.820
	VASP-GGA [8]	3.899	249	408	170	180	152	1.633
	TB-LMTO [13]	3.837	326.3					
	TB-LMTO-GGA [28]	3.88	300	449.7	225.1	109.5		
	TB-LMTO-LDA [28]	3.82	308.5	486.07	219.8	140.3		
	Exp. [13]	3.861						
	Exp. [24]	3.860						
	Exp. [25]	3.860						
	Exp. [26]	3.860						
	[29]		256					

using the VASP–GGA method. The values agree reasonably well. An important material parameter is the *B/G* ratio, as an indication of ductility and brittleness. According to the Pugh criteria [45], a high *B/G* ratio indicates ductility, while a low *B/G* ratio indicates brittleness. The critical value, separating ductile materials from brittle ones, is 1.75. We have calculated the ratio for Ir_3Ta and Rh_3Ta alloys and found values of *B/G* for Ir_3Ta of 1.522 by the GGA method and 1.669 by LDA, while for Rh_3Ta the ratio is 1.702 by GGA and 1.820 by LDA. The calculated values of *B/G* for LDA are larger than the computed GGA values for both alloys. The results of LDA and GGA calculations for the lattice constants indicate that LDA values are smaller than GGA values. Hence, while calculated values within the LDA are closer to the experimental data, GGA calculations predict a too large lattice constant. Ir_3Ta exhibit a brittle nature for these *B/G* values. The ratio for the Rh_3Ta is less than 1.75 from GGA and it increases with LDA. These results suggest that Rh_3Ta is prone to brittleness from GGA, and is slightly prone to ductility from LDA. Thus, there is a further need for experimental work to compare with our *B/G* ratios for Rh_3Ta.

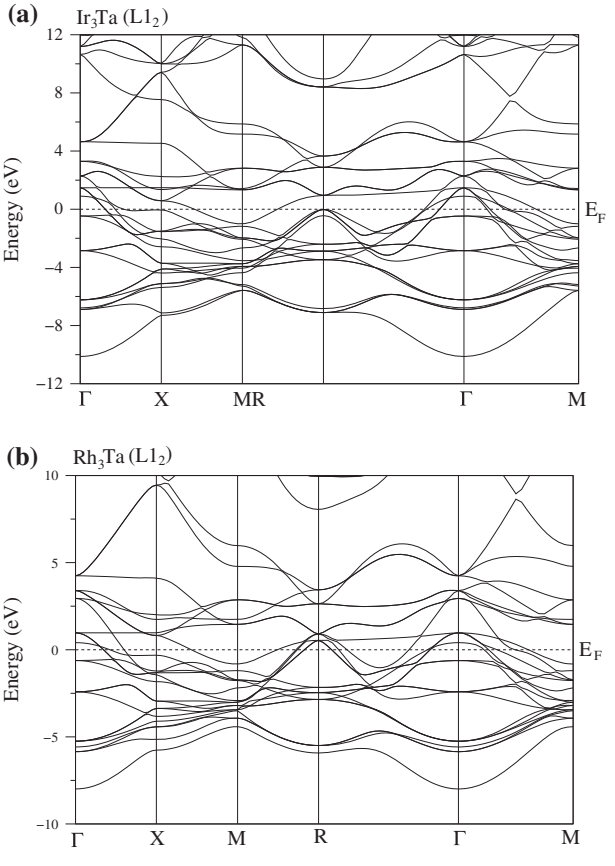

Figure 1. Electronic band structure of Ir_3Ta and Rh_3Ta.

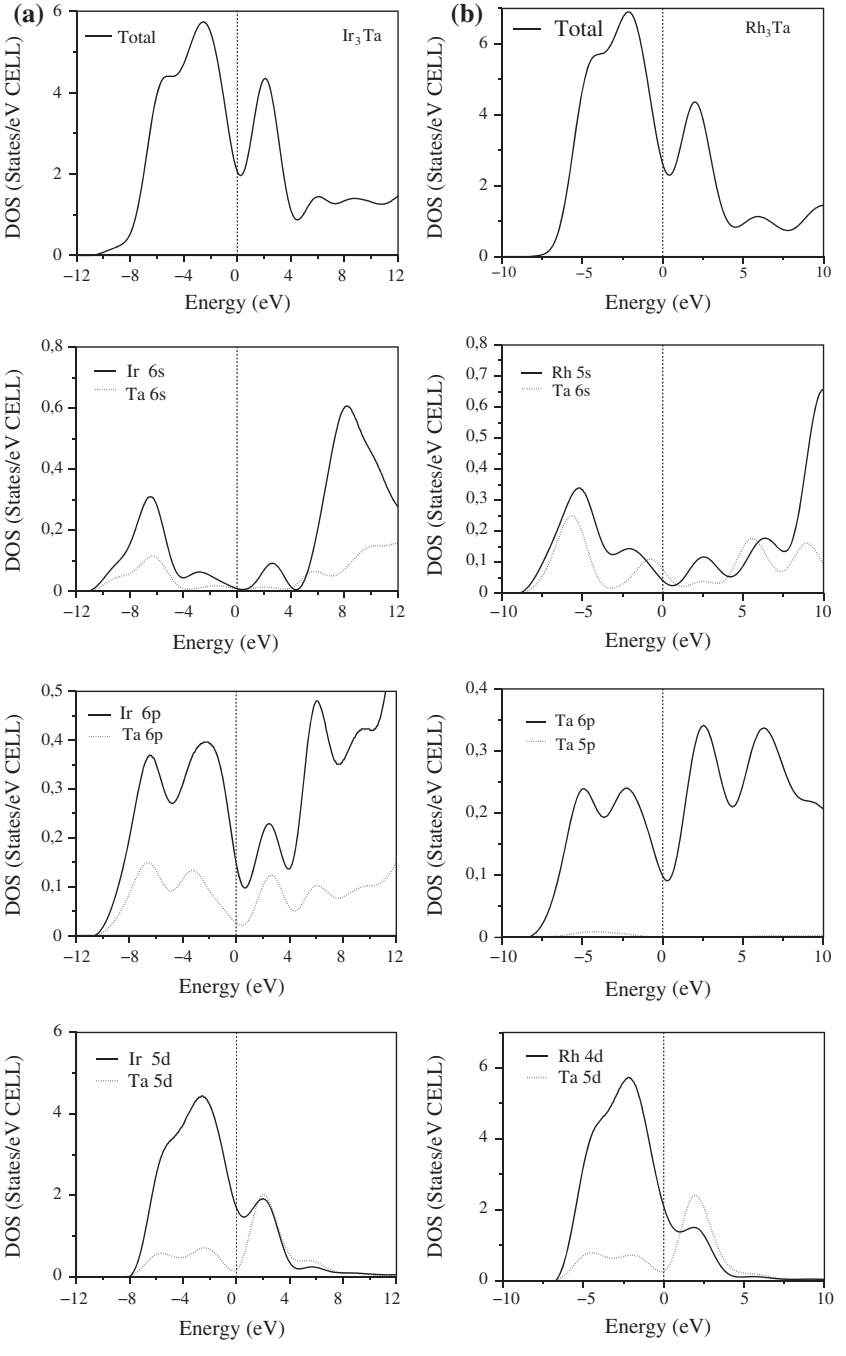

Figure 2. Total and partial densities of states of (a) Ir_3Ta and (b) Rh_3Ta.

Figure 1a and b shows the energy band structures of Ir_3Ta and Rh_3Ta alloys in the $L1_2$ phase. Both alloys have metallic character because there is no gap at the Fermi level. Our presented band structures for Ir_3Ta and Rh_3Ta alloys are in good agreement with previously reported results [13,14,23]. The character of the band states has been identified using the calculated total and partial densities of states (DOS) for the alloys (in Figure 2a and b). The features in the total DOS for Ir_3Ta and Rh_3Ta look similar. Our calculated total DOS is in good agreement with those previously reported [13,14]. In Figure 1a and b, the bottom bands of Ir_3Ta and Rh_3Ta alloys mainly come from Ir-5d states and Rh-4d states, respectively. The electronic density of states (Figure 2a and b) around the Fermi level is due to Ir-5d states for Ir_3Ta and Rh-4d states for Rh_3Ta. Part of these bands is unoccupied and the total DOS shows pseudogaps near the Fermi level. The contribution of one peak, around 2 eV above the Fermi level, is by partially filled or antibonding states, dominated by Ir-5d states and Ta-5d states for Ir_3Ta, and Rh-4d states and Ta-5d states for Rh_3Ta, which is consistent with previous calculations [13,14]. We have calculated the density of states at the Fermi level $N(E_F)$. These are 2.07 and 2.64 states/eV cell for Ir_3Ta and Rh_3Ta, respectively.

The $L1_2$ structure of Ir_3Ta and Rh_3Ta alloys contains four ions in the unit cell, and hence there are 12 modes for each wave vector $\boldsymbol{q}$. Using the GGA (QE) and LDA (VASP) in the $L1_2$ phase, we calculated the phonon properties for these alloys. In Figure 3a and b, the calculated phonon dispersion curves and corresponding density of states (DOS), including the partial density of states and total density of states of Ir_3Ta and Rh_3Ta, are displayed. The figure also shows the main characters of the vibration modes. Since the phonon frequencies ω, along all directions in the Brillouin zone, are not imaginary, the phonon spectra illustrate that Ir_3Ta and Rh_3Ta alloys are dynamically stable. There is no separation of optic modes from acoustic ones for either alloy. In Figure 3a and b, we see that the vibrations of Ir atoms compose the highest frequency region of both alloys. We find that the partial density of states is mostly constituted of Ir (Rh) and Ta atoms in acoustic modes. For Ir_3Ta, we calculated the Γ-point optical phonon modes to be 3.574, 4.078 and 5.347 THz, and for Rh_3Ta as 3.516, 5.075 and 6.922 THz, using linear response theory. Using VASP code (direct method), the values were for Ir_3Ta, 3.828, 4.119 and 5.522 THz, and for Rh_3Ta, 3.861, 5.573 and 7.157 THz). It is to be noted that the values of Γ-point optical phonon frequencies computed by the linear response method are slightly lower than those computed by the direct method. We have observed the same behaviour for the GGA and LDA phonon dispersion relationship for both alloys. No theoretical and experimental data are available for comparison.

The QHA based on DFPT includes important information for the thermodynamic properties of materials. The temperature dependence of the vibrational contributions to the specific heat capacity at constant volume, C_V, in QHA is as follows:

$$C_V = \sum_{q\lambda} k_B \left(\frac{\hbar\omega_{q\lambda}(V)}{2k_BT}\right)^2 cosh^2\left(\frac{\hbar\omega_{q\lambda}(V)}{k_BT}\right)^2$$

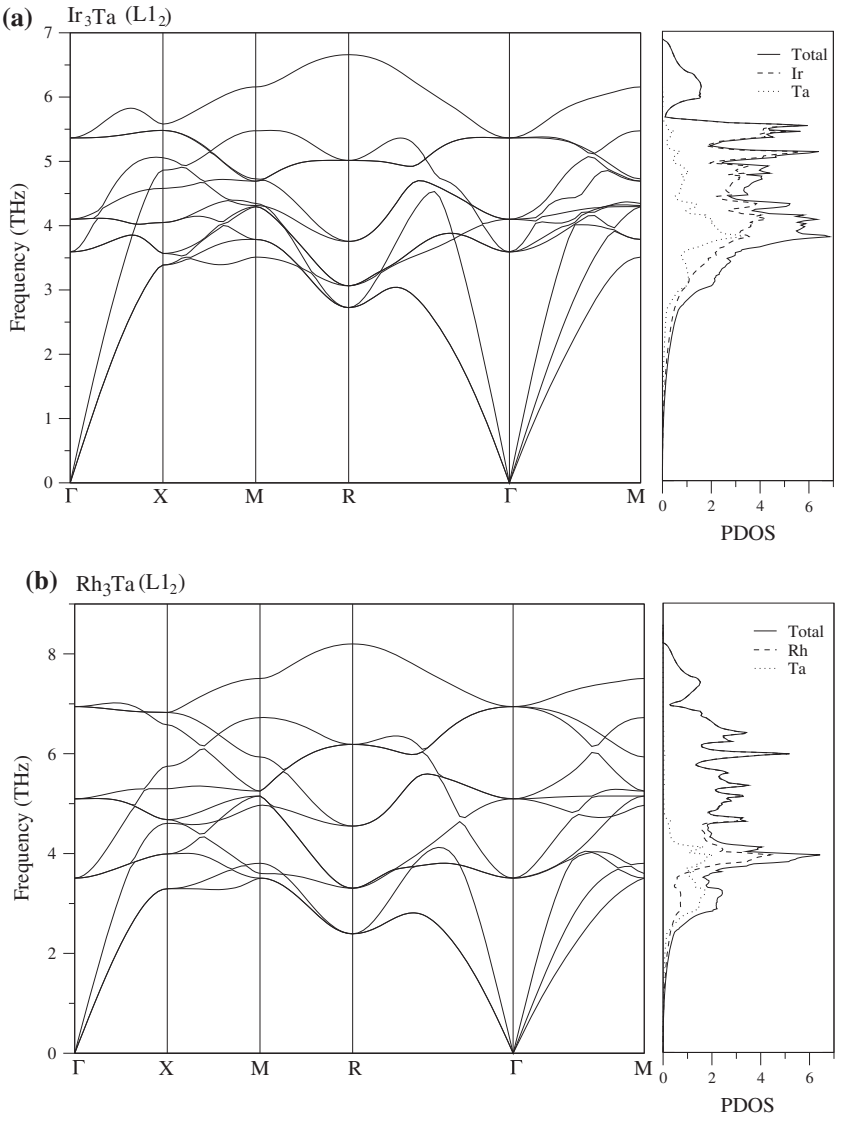

Figure 3. Phonon dispersion curves and DOS of (a) Ir_3Ta and (b) Rh_3Ta.

In this work, the specific heat capacity at constant volume is taken to consist of the phonon contribution. Figure 4 shows the temperature dependence of specific heat for the Ir_3Ta and Rh_3Ta alloys. The specific heat capacities increase rapidly up to 200 K with increasing temperature. At higher temperatures, the computed specific heat capacity can take values above the Dulong–Petit limit [46]. Unfortunately, experimental data for the specific heat capacity of these materials are not available in the literature.

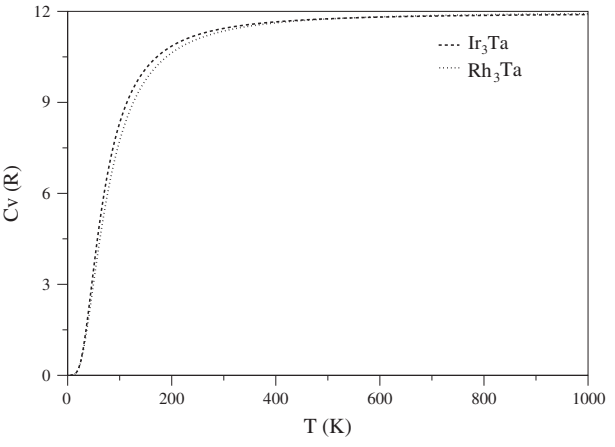

Figure 4. Calculated specific heat capacity at constant volume vs. temperature for the Ir_3Ta and Rh_3Ta alloys in the $L1_2$ structure.

Conclusions

In summary, we have performed *ab initio* calculations to study the structural, elastic, electronic, dynamical and thermodynamic properties of Ir_3Ta and Rh_3Ta alloys in the $L1_2$ phase. Our calculated structural and elastic properties are in reasonable agreement with the available theoretical results and experimental data. Band structures and density of states calculations confirm the metallicity of the Ir_3Ta and Rh_3Ta alloys in the $L1_2$ phase. Finally, we have calculated the phonon frequencies using different approximations.

Disclosure statement

No potential conflict of interest was reported by the authors.

References

[1] Y. Yamabe-Mitarai, Y. Ro, T. Maruko, T. Yokokawa and H. Harada, Defects Diffus. Forum 188–190 (2001) p.171.
[2] Y. Yamabe-Mitarai, Y. Koizumi, H. Murakami, Y. Ro, T. Maruko and H. Harada, Scr. Mater. 36 (1997) p.393–398.
[3] Y. Yamabe-Mitarai, Y. Ro, T. Maruko and H. Harada, Metall. Mater. Trans. A 29 (1998) p.537–549.
[4] E. Watanabe, Y. Abe, K. Sasaki and S. Iura, Vacuum 74 (2004) p.735–739.
[5] C. Huang, Y. Yamabe-Mitarai, S. Nakazawa, K. Nishida and H. Harada, Mater. Sci. Eng. A 412 (2005) p.191–197.
[6] S. Miura, K. Honma, Y. Terada, J.M. Sanchez and T. Mohri, Intermetallics 8 (2000) p.785–791.
[7] V.E. Nuttens, R.L. Hubert, F. Bodart and S. Lucas, Nucl. Instrum. Methods Phys. Res. Sect. B 240 (2005) p.425–428.
[8] K. Chen, L.R. Zhao, J.S. Tse and J.R. Rodgers, Phys. Lett. A 331 (2004) p.400–403.
[9] Y. Terada, K. Ohkubo, S. Miura, J.M. Sanchez and T. Mohri, Mater. Chem. Phys. 80 (2003) p.385–390.

[10] Y. Terada, K. Ohkubo, S. Miura, J.M. Sanchez and T. Mohri, J. Alloys Compd. 354 (2003) p.202–207.
[11] Y. Terada, Platinum Met. Rev. 52 (2008) p.208–214.
[12] X. Yu, Y. Yamabe-Mitarai, Y. Ro, Y. Gu and H. Harada, Scr. Mater. 41 (1999) p.651–657.
[13] M. Rajagopalan and M. Sundareswari, J. Alloys Compd. 379 (2004) p.8–15.
[14] M. Sundareswarı and M. Rajagopalan, Int. J. Mod. Phys. B 19 (2005) p.4587–4604.
[15] S. Miura, K. Ohkubo, Y. Terada, Y. Kimura, Y. Mishima, Y. Yamabe-Mitarai, H. Harada and T. Mohri, J. Alloys Compd. 395 (2005) p.263–271.
[16] C. Huang, Y. Yamabe-Mitarai, X.H. Yu and H. Harada, Intermetallics 12 (2004) p.619–623.
[17] M. Sundareswari and M. Rajagopalan, Physica B 403 (2008) p.2530–2541.
[18] M. Sluiter, P. Turchi and D. Fontaine, J. Phys. F: Met. Phys. 17 (1987) p.2163–2178.
[19] Y. Yamabe-Mitarai, Y. Ro and S. Nakazawa, Intermetallics 9 (2001) p.423–429.
[20] S.V. Meschel, X.Q. Chen, O.J. Kleppa and P. Nash, Calphad 33 (2009) p.55–62.
[21] N. Dalili, Q. Liu and D.G. Ivey, Acta Mater. 61 (2013) p.5365–5374.
[22] K. Chen, L.R. Zhao and J.S. Tse, J. Appl. Phys. 93 (2003) p.2414–2417.
[23] O.Y. Kontsevoi, Y.N. Gornostyrev, A.F. Maksyutov, K.Y. Khromov and A.J. Freeman, Metall. Mater. Trans. A 36 (2005) p.559–566.
[24] A.E. Dwight and P.A. Beck, Trans. Metall. Soc. AIME 215 (1959) p.976–979.
[25] H. Kleykamp, J. Less-Common Met. 152 (1989) p.15–24.
[26] B.C. Giessen, H. Ibach and N.J. Grant, Trans. Metall. Soc. AIME 230 (1964) p.113–122.
[27] W.H. Jr. Ferguson, B.C. Giessen and N.J. Grant, Trans. Metall. Soc. AIME 227 (1963) p.1401–1406.
[28] M. Ould Kada, T. Seddik, A. Sayede, R. Khenata, A. Bouhemadou, E. Deligöz, Z.A. Alahmed, S. Bin Omran and D. Rached, Int. J. Mod. Phys. B 28 (2014) 1450006 p.1–17.
[29] O.Y. Kontsevoi, Y.N. Gornostyrev and A.J. Freeman, JOM 57 (2005) p.43–47.
[30] P. Giannozzi, S. Baroni, N. Bonini, M. Calandra, R. Car, C. Cavazzoni, D. Ceresoli, G.L. Chiarotti, M. Cococcioni, I. Dabo, A. Dal Corso, S. Fabris, G. Fratesi, S. de Gironcoli, R. Gebauer, U. Gerstmann, C. Gougoussis, A. Kokalj, M. Lazzeri, L. Martin-Samos, N. Marzari, F. Mauri, R. Mazzarello, S. Paolini, A. Pasquarello, L. Paulatto, C. Sbraccia, S. Scandolo, G. Sclauzero, A.P. Seitsonen, A. Smogunov, P. Umari and R.M. Wentzcovitch, J. Phys.: Condens. Matter 21 (2009) 395502 p.1–19.
[31] G. Kresse and J. Hafner, Phys. Rev. B 48 (1993) 13115–13118.
[32] G. Kresse and J. Furthmüller, Comput. Mater. Sci 6 (1996) 145; Phys. Rev. B 54 (1996) 11169–11186.
[33] P. Perdew, K. Burke and M. Ernzerhof, Phys. Rev. Lett. 77 (1996) p.3865–3868.
[34] J.P. Perdew and A. Zunger, Phys. Rev. B 23 (1981) p.5048–5079.
[35] P.E. Blöchl, Phys. Rev. B 50 (1994) p.17953–17979.
[36] G. Kresse and D. Joubert, Phys. Rev. B 59 (1999) p.1758–1775.
[37] H.J. Monkhorst and J.D. Pack, Phys. Rev. B 13 (1976) p.5188–5192.
[38] M. Methfessel and A.T. Paxton, Phys. Rev. B 40 (1989) p.3616–3621.
[39] S. Baroni, P. Giannozzi and A. Testa, Phys. Rev. Lett. 58 (1987) p.1861–1864.
[40] S. Baroni, S. del Gironcoli, A. Dal Corsa and P. Giannozzi, Rev. Mod. Phys. 73 (2000) p.515–562.
[41] K. Parlinski, Z.Q. Li and Y. Kawazoe, Phys. Rev. Lett. 78 (1997) p.4063–4066.
[42] E. Isaev (2009) Qha: Calculation of Thermodynamic Properties Using the Quasi-Harmonic Approximation. Available at http://qha.qe-forge.org. Accessed 22 Jul 2013.
[43] N. Arıkan, Z. Charifi, H. Baaziz, Ş. Uğur, H. Ünver and G. Uğur, J. Phys. Chem. Solids 77 (2015) p.126–132.
[44] Ş. Uğur, N. Arıkan, F. Soyalp and G. Uğur, Comput. Mater. Sci. 48 (2010) p.866–870.
[45] S.F. Pugh, Philos. Mag. 45 (1954) p.823–843.
[46] A.T. Petit and P.L. Dulong, Ann. Chim. Phys. 10 (1819) p.395–413.